

Asymmetric Synthesis and in Vitro and in Vivo Activity of Tetrahydroquinolines Featuring a Diverse Set of Polar Substitutions at the 6 Position as Mixed-Efficacy μ Opioid Receptor/ δ Opioid Receptor Ligands

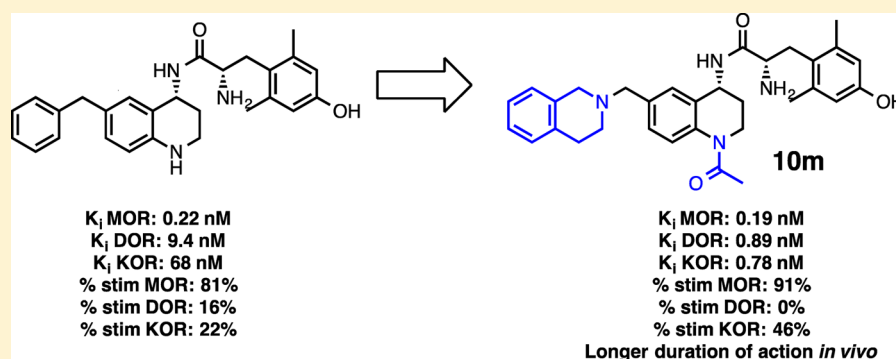
Aaron M. Bender,[†] Nicholas W. Griggs,[‡] Jessica P. Anand,[‡] John R. Traynor,[‡] Emily M. Jutkiewicz,[‡] and Henry I. Mosberg^{*,†,§}

[†]Interdepartmental Program in Medicinal Chemistry, College of Pharmacy, University of Michigan, Ann Arbor, Michigan 48109, United States

[‡]Department of Pharmacology, School of Medicine, University of Michigan, Ann Arbor, Michigan 48109, United States

[§]Department of Medicinal Chemistry, College of Pharmacy, University of Michigan, Ann Arbor, Michigan 48109, United States

S Supporting Information



ABSTRACT: We previously reported a small series of mixed-efficacy μ opioid receptor (MOR) agonist/ δ opioid receptor (DOR) antagonist peptidomimetics featuring a tetrahydroquinoline scaffold and showed the promise of this series as effective analgesics after intraperitoneal administration in mice. We report here an expanded structure–activity relationship study of the pendant region of these compounds and focus in particular on the incorporation of heteroatoms into this side chain. These analogues provide new insight into the binding requirements for this scaffold at MOR, DOR, and the κ opioid receptor (KOR), and several of them (**10j**, **10k**, **10m**, and **10n**) significantly improve upon the overall MOR agonist/DOR antagonist profile of our previous compounds. *In vivo* data for **10j**, **10k**, **10m**, and **10n** are also reported and show the antinociceptive potency and duration of action of compounds **10j** and **10m** to be comparable to those of morphine.

KEYWORDS: Opioid, mixed efficacy, intraperitoneal, dependence, tolerance, tetrahydroquinoline

Opioid analgesics have long been the standard for the treatment of severe pain. Unfortunately, the use of opioids can lead to the development of a number of undesirable side effects, such as respiratory depression, constipation, and perhaps most problematically, dependence and tolerance.¹ There is therefore a great unmet need to develop agents that act as potent analgesics but without the development of these side effects.^{2,3}

There is a growing body of evidence to suggest that the δ opioid receptor (DOR) plays a significant role in the modulation of the side effects related to the chronic use of opioid analgesics. Although the analgesic effects of traditional opioid agents such as morphine are associated with stimulation of the μ opioid receptor (MOR), the coadministration of DOR antagonists has been shown to maintain the desired

antinociceptive activity but with a reduced side-effect profile compared with a MOR agonist alone.^{4–7}

Because of these findings, our group and others have sought to develop bifunctional ligands that bind to both MOR and DOR but stimulate only MOR. Several classes of compounds have been employed in this pursuit, including peptides,⁸ pseudopeptides,^{9,10} and small molecules.^{11,12} The MOR/DOR bivalent ligands developed by Portoghese and colleagues have been demonstrated to be effective analgesics with a diminished tolerance profile (Figure 1d),¹³ and recently the MOR/DOR heteromer-biased agonist CYMS1010 was also shown to display

Received: March 25, 2015

Revised: May 1, 2015

Published: May 4, 2015

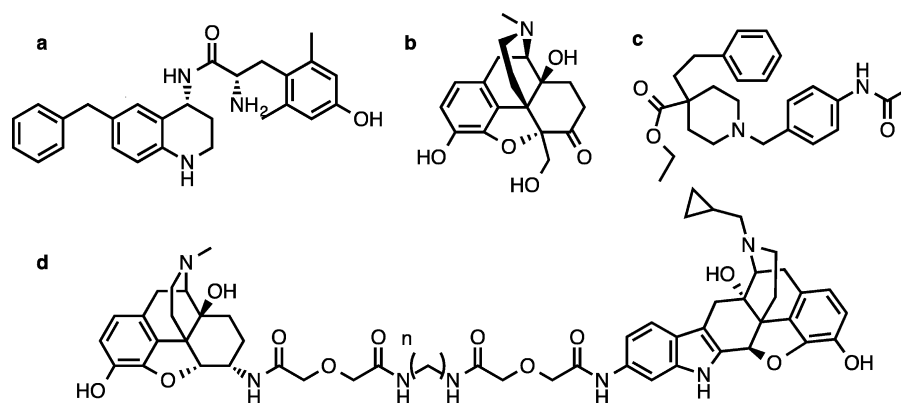
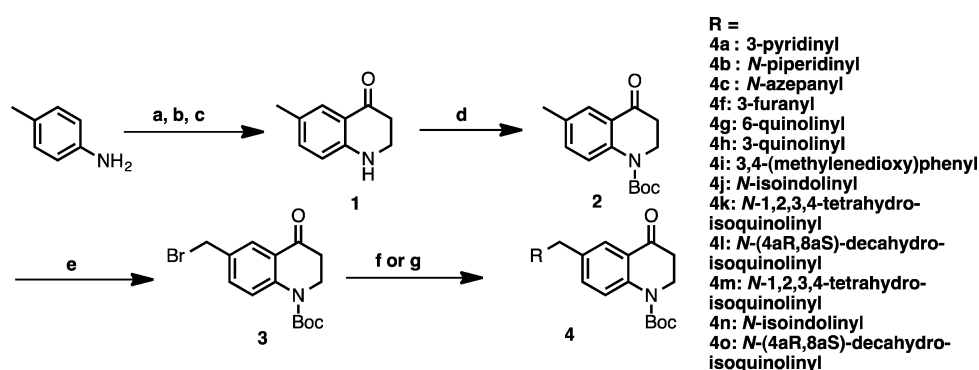


Figure 1. Bifunctional MOR/DOR ligands. Compound **a** is from ref 17.

Scheme 1. Synthesis of Intermediates 4a–c,f–o^a



^aReagents and conditions: (a) 3-bromopropionyl chloride, K_2CO_3 , DCM, r.t.; (b) NaOtBu, DMF, r.t.; (c) TfOH, DCE, r.t.; (d) $(Boc)_2O$, DMAP, DIPEA, DCM, reflux; (e) NBS, benzoyl peroxide, CCl_4 , reflux; (f) boronic acid or pinacol ester, $Pd(dppf)Cl_2$, K_2CO_3 , acetone, water, 100 °C with microwave irradiation; (g) secondary amine, K_2CO_3 , DMF, r.t.

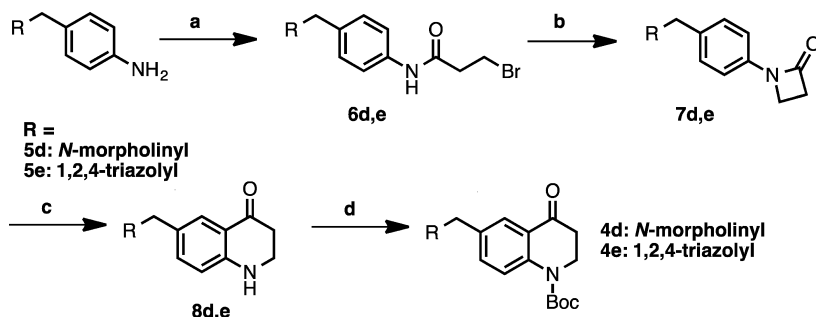
reduced antinociceptive tolerance compared with morphine (Figure 1c).¹⁴ MOR agonist/DOR antagonist compounds are also being developed clinically for the treatment of irritable bowel syndrome.¹⁵ We have recently reported two MOR agonist/DOR antagonist compounds that are effective and bioavailable analgesics: a glycosylated cyclic pentapeptide¹⁶ and a small molecule with a tetrahydroquinoline (THQ) core (Figure 1a).^{17,18} Additionally, UMB425, a small-molecule MOR agonist/DOR antagonist derived from thebaine, was reported to display analgesia after subcutaneous administration with reduced tolerance compared with morphine (Figure 1b).¹⁹

The compounds reported in this paper build on the limited initial structure–activity relationship (SAR) study done on our bioavailable THQ lead compound (*S*)-2-amino-*N*-((*R*)-6-benzyl-1,2,3,4-tetrahydroquinolin-4-yl)-3-(4-hydroxy-2,6-dimethylphenyl)propanamide (**a** in Figure 1a). Initially, bulky hydrophobic modifications to the side chain at position R_1 (see Table 1) were examined,¹⁷ as these substitutions were directly comparable to a previously reported series of MOR/DOR cyclic peptides^{20,21} and were hypothesized to interact favorably with residues in the MOR active pocket to act as full MOR agonists while simultaneously behaving as DOR antagonists. These initial compounds were highly lipophilic, which is desirable for blood–brain barrier penetration but less than optimal for both aqueous solubility and metabolic stability.²² We therefore explored a variety of polar side chains on this scaffold for the purpose of improving these parameters and further probing the chemical space in this region of each of the

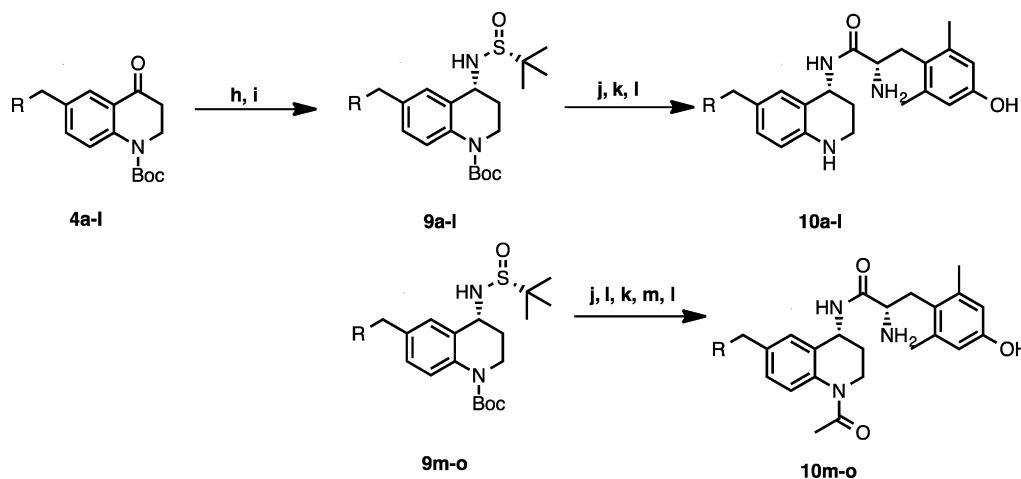
receptors. Simple heteroatom replacements not only had profound effects on receptor selectivity but also led to compounds that improved upon the *in vivo* profile of our initial THQ analogue. Compounds **10j** and **10m** both produced a maximum antinociceptive response in the mouse warm water tail withdrawal (WWTW) assay, and both improved significantly upon the duration of action of our lead peptidomimetic. These findings highlight the promise of this scaffold *in vivo* and show that our SAR strategy focusing on polar side chains was effective for improving bioavailability. *In vitro* data for both binding affinity and efficacy are presented for all three opioid receptor types (MOR, DOR, and the κ opioid receptor (KOR)).

RESULTS AND DISCUSSION

Chemistry. The synthesis of compounds **10a–c,f–o** began with the acylation of *p*-toluidine with 3-bromopropionyl chloride (Scheme 1). The resulting alkyl bromide then underwent an intramolecular cyclization followed by triflic acid-mediated β -lactam rearrangement to give ketone **1**,^{23,24} which was subsequently Boc-protected on the THQ nitrogen to give **2**. Ketone **2** was then brominated on the aryl methyl group as described previously²⁵ to give **3**, onto which could be added the pendant of choice, through either Suzuki coupling (**4a,f–i**) or substitution with the appropriate secondary amine (**4b,c,j–o**). It is important to note that **3** could be synthesized on a multigram scale and that all substitutions on this intermediate were high-yielding. For the synthesis of compounds **10d** and

Scheme 2. Synthesis of Intermediates 4d and 4e^a

^aReagents and conditions: (a) 3-bromopropionyl chloride, K₂CO₃, DCM, r.t.; (b) NaOtBu, DMF, r.t.; (c) TfOH, DCE, r.t.; (d) (Boc)₂O, DMAP, DIPEA, DCM, reflux.

Scheme 3. Final Steps in the Synthesis of 10a–o^a

^aReagents and conditions: (h) (*R*)-(+)-2-methyl-2-propanesulfonamide, Ti(OEt)₄, THF, reflux; (i) NaBH₄, THF; (j) conc. HCl, 1,4-dioxane, r.t.; (k) Boc-*L*-Dmt, PyBOP, DIPEA, HOBT-Cl, DMF, r.t.; (l) TFA, DCM, r.t.; (m) (Ac)₂O, pyridine, r.t.

10e, commercially available para-substituted anilines were carried forward in a similar manner as in the synthesis of compound **2** to give intermediates **4d** and **4e** (Scheme 2).

Ketones **4a–o** were converted to the corresponding imines with (*R*)-(+)-2-methyl-2-propanesulfonamide and Ti(OEt)₄ and could then be reduced asymmetrically with NaBH₄ in situ to give *tert*-butanesulfinyl-protected amines **9a–o** as single diastereomers (Scheme 3), as previously described for analogous scaffolds.^{26,27} Deprotection with concentrated HCl gave the corresponding primary, enantiomerically pure (*R*)-amines as HCl salts. The stereochemistry of the HCl salts was verified by X-ray crystallography of 6-benzyl-1-(*tert*-butoxycarbonyl)-1,2,3,4-tetrahydroquinolin-4-aminium chloride, which was prepared by an identical synthetic route (Figure 2).

Boc-protected *L*-2,6-dimethyltyrosine (Boc-*L*-Dmt) could then be coupled to the chiral HCl salt, and subsequent deprotection with trifluoroacetic acid (TFA) afforded **10a–l** (Scheme 3). The analogues were then purified by reversed-phase (RP) HPLC to provide enough material for in vitro and in vivo pharmacological evaluation (~5–10 mg). In the case of the *N*-acetylated analogues **10m–o**, Boc deprotection of the THQ nitrogen was performed prior to coupling to Boc-*L*-Dmt. After the amide coupling, the acetyl group was introduced by stirring the crude material in excess pyridine/acetic anhydride (1:1) overnight, followed by a second Boc deprotection and RP-HPLC purification. The TFA content of the final analogues

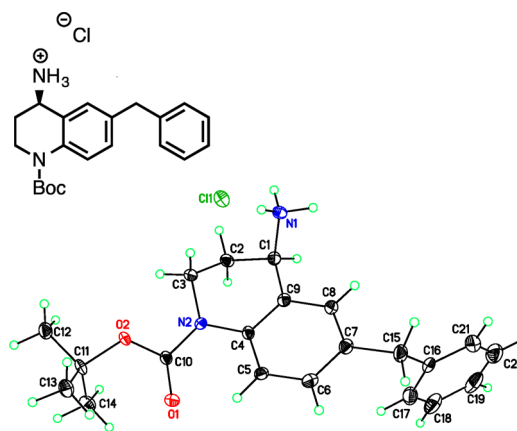


Figure 2. Crystal structure of (*R*)-6-benzyl-1-(*tert*-butoxycarbonyl)-1,2,3,4-tetrahydroquinolin-4-aminium chloride.

was estimated by ¹⁹F NMR analysis as described previously using a fluorinated analogue of **10m** (see the Supporting Information) and was found to be approximately 2.5 TFA molecules per molecule of final compound.²⁸

SAR Studies. In previous reports, we described a mixed-efficacy MOR agonist/DOR antagonist opioid peptidomimetic featuring a THQ scaffold and a benzyl pendant at ring position 6^{17,18} (**a** in Figure 1a). This compound was shown to be an

effective analgesic in the WWTW assay after intraperitoneal administration, with a duration of action slightly shorter than that of morphine.¹⁷ The initial SAR study done on this lead compound was focused on several additional hydrophobic, aromatic substitutions at the 6 position, including 1-methylnaphthyl, 2-methylnaphthyl, 2-methylindanyl, and ethylphenyl. The side chains of these four compounds were chosen to mirror modifications made in a peptide series upon which the peptidomimetic scaffold was based,²⁰ and as expected, modifications featuring a more extended pendant (2-methylnaphthyl, 2-methylindanyl, ethylphenyl) were compatible with the larger DOR *inactive* binding pocket but not the smaller DOR *active* pocket, explaining the observed low efficacy at DOR. While these compounds displayed the desired MOR agonist/DOR antagonist efficacy profile, their binding profile was not optimal. The MOR affinity for all four compounds was at least an order of magnitude higher than the DOR affinity, and the 2-methylnaphthyl compound showed an over 2 orders of magnitude preference for MOR. Ligands with more balanced binding affinities at MOR and DOR would provide a better starting point for further development of this type of mixed-efficacy opioid ligand.^{9,30} Additionally, although we showed that an extended hydrophobic pendant translates to low DOR efficacy, changes in the electronic characteristics and polarity of the pendant were left unexplored.

To begin our expanded SAR, we first replaced the phenyl pendant of our lead compound (Figure 1a) with a 3-pyridine (10a; Table 1). We observed not only a slight loss in binding affinity (K_i) at both MOR and DOR (Table 1) but also a significant loss in MOR efficacy (EC_{50}) and potency (as maximal % stimulation) (Table 2) (see Methods for details of the *in vitro* assays). Although 10a adopts a similar conformation as our lead compound in the MOR active site, this loss in MOR binding and efficacy can be attributed to loss of hydrophobic contacts in this region of the receptor binding pocket (see Figure 3). Although this analogue did not improve upon the MOR agonist/DOR antagonist profile of our previous compounds, we were intrigued by the drastic consequences that a simple change in pendant electronics had on both the binding and efficacy and wished to explore this further. Compared with 10a and our lead compound, replacement with piperidine in analogue 10b widened the binding affinity preference for MOR over DOR even further, although this compound behaved as a moderately potent full agonist at MOR, improving upon the MOR efficacy profile of 10a. Expansion of the piperidine ring in 10b to azepane (10c) resulted in improved binding at DOR and KOR. In contrast, the morpholine analogue 10d displayed diminished binding affinities at DOR and KOR and also decreased potency at MOR compared with 10b. We next turned our attention to smaller aromatic systems, including 1,2,4-triazole (10e) and 3-furan (10f). While the overall binding profile of 10f was comparable to those for the previous substitutions, 10e displayed a marked loss in binding affinity for MOR and KOR and displayed no efficacy at MOR.

In the initial series,¹⁷ the 2-methylnaphthyl modification resulted in the highest MOR efficacy, but the MOR/DOR binding balance favored MOR by over 2 orders of magnitude. To see whether changes in the electronics of the naphthyl system could improve DOR binding while maintaining low DOR efficacy, we first synthesized quinoline analogue 10g. Interestingly, the binding affinities of 6-quinoline analogue 10g at all three receptors were considerably lower than those of the previous bicyclic analogues. This finding suggests that both an

Table 1. Opioid Receptor Binding Affinities and $\log P^c$ Values for Analogues 10a–o^a

Compound	R ₁	R ₂	Binding, K_i (nM)			$\log P^c$
			MOR	DOR	KOR	
(Fig 1a)		H	0.22±0.02 ^b	9.4±0.8 ^b	68±2 ^b	3.7
10a		H	0.66±0.08	17±4	66±8	2.2
10b		H	0.3±0.1	120±29	29±9	2.7
10c		H	0.15±0.02	61±9	3.6±0.7	3.3
10d		H	0.6±0.1	140±67	170±32	1.4
10e		H	3.1±0.6	50±14	450±14	0.75
10f		H	0.8±0.2	18±6	20±3	2.9
10g		H	2.1±0.6	23±5	120±21	3.6
10h		H	0.10±0.02	1.5±0.2	16±4	3.6
10i		H	0.12±0.01	4.3±0.8	21±2	3.7
10j		H	0.15±0.08	15±5	2±1	3.1
10k		H	0.03±0.01	3.1±0.2	2.2±0.4	3.6
10l		H	0.15±0.01	4.8±0.9	37±8	4.1
10m		Acetyl	0.19±0.1	0.89±0.2	0.78±0.1	3.2
10n		Acetyl	0.32±0.09	2.6±0.2	7±3	2.7
10o		Acetyl	0.8±0.2	2±1	15±6	3.7

^aBinding affinities (K_i) were obtained by competitive displacement of [³H]diprenorphine in membrane preparations expressing either MOR, DOR, or KOR. All values are mean ± standard error of the mean (SEM) of three separate assays performed in duplicate. ^bData from ref 17. ^cCalculated using ChemBioDraw Ultra, version 14.0.

extended pendant and pendant electronic characteristics are important for maintaining binding at DOR for this series. Using our previously published models of interactions of opioid ligands with the active states of the three receptors,^{20,21} we docked 10g into the MOR active binding pocket. The quinoline nitrogen of 10g was found to extend much deeper into the hydrophobic pocket of the MOR active pocket, disrupting important contacts with hydrophobic residues W133, V143, and I144, as shown in Figure 3.

These initial data suggested that superior MOR efficacy (and low DOR efficacy) may result from a fused-ring pendant in which the six-membered non-heteroatom-containing aromatic moiety is located in the position most distal from the THQ

Table 2. Opioid Receptor Efficacies for Analogues 10a–o^a

compound	EC ₅₀ (nM)			% stimulation		
	MOR	DOR	KOR	MOR	DOR	KOR
a (Fig. 1)	1.6 ± 0.3 ^b	110 ± 6 ^b	540 ± 72 ^b	81 ± 2 ^b	16 ± 2 ^b	22 ± 2 ^b
10a	93 ± 20	dns	dns	37 ± 7	dns	dns
10b	9 ± 1	dns	dns	73 ± 8	dns	dns
10c	25 ± 11	dns	dns	52 ± 2	dns	dns
10d	60 ± 2	dns	dns	82 ± 2	dns	dns
10e	dns	dns	dns	dns	dns	dns
10f	72 ± 24	dns	>1000	18 ± 2	dns	>40
10g	23 ± 13	dns	dns	34 ± 6	dns	dns
10h	2.2 ± 0.9	dns	dns	84 ± 6	dns	dns
10i	14 ± 3	dns	dns	36 ± 3	dns	dns
10j	3 ± 1	dns	15 ± 9	96 ± 4	dns	14 ± 2
10k	0.4 ± 0.1	dns	90 ± 65	105 ± 6	dns	25 ± 4
10l	2.0 ± 0.5	dns	600 ± 400	56 ± 2	dns	14 ± 1
10m	6 ± 2	dns	160 ± 36	91 ± 8	dns	46 ± 5
10n	0.9 ± 0.4	dns	400 ± 130	118 ± 5	dns	32 ± 1
10o	40 ± 20	dns	>2000	72 ± 3	dns	>20

^aEfficacy data were obtained using agonist-induced stimulation of [³⁵S]GTPγS binding in membrane preparations expressing either MOR, DOR, or KOR. Potencies are represented as EC₅₀ (nM) and efficacies as percent maximal stimulation relative to the standard agonist DAMGO (MOR), DPDPE (DOR), or U69,593 (KOR) at 10 μM. All values are expressed as the mean ± SEM of three separate assays performed in duplicate. dns: does not stimulate. ^bData from ref 17.

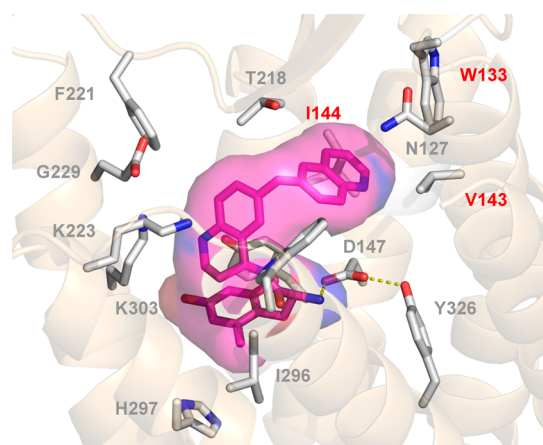


Figure 3. Docking of **10g** in the MOR active site. Key hydrophobic contacts (I144, V143, W133) are highlighted in red.

core. To test this hypothesis, analogues **10h–l** were synthesized. **10h** showed high efficacy at MOR and approximately 10-fold improved DOR binding compared with the lead compound and **10g**. **10j** and **10k** both behaved as potent full MOR agonists that improved upon the efficacy of our original lead with no efficacy at DOR. On the other hand, the MOR efficacy was reduced in the case of 3,4-(methylenedioxy)phenyl analogue **10i**. This is again consistent with the observation that distal electron rich substitutions adversely affect the MOR efficacy. Reduction of the aromatic ring of **10k** to give decahydroisoquinoline analogue **10l** maintained a comparable but slightly inferior in vitro profile compared with **10k**. While **10j** and **10k** showed potent stimulation at MOR (while exhibiting no efficacy at DOR), we still wished to improve the binding affinities of each at DOR. We reasoned that the THQ aniline was synthetically accessible and amenable to substitutions and would be the next logical site for diversification. Preliminary studies on related analogues (to be published in due course) suggested that N-acetylation at the

THQ core improves DOR affinity without increasing DOR efficacy, so we likewise explored the effect of an acetyl substituent here, giving the final analogues **10m–o**. We were pleased to see not only that this modification improved DOR binding relative to the unacetylated counterpart compounds (**10j–l**) but also that **10m** showed similarly high affinity for MOR and DOR and, interestingly, for KOR as well. As expected from its high binding affinity and lack of stimulation of [³⁵S]GTPγS binding, **10m** acted as an antagonist of DPDPE. **10m** afforded a 7.8-fold rightward shift in the agonist concentration–response curve for DPDPE, giving an antagonist affinity constant (K_e) of 4.6 nM for **10m**.

An overlay of **10k** docked into the active sites of all three receptors is shown in Figure 4. The compound fits nicely into the MOR active site but clashes with M199 and L125 in the DOR active site. It is interesting to note that **10k** and **10m**, both featuring the 1,2,3,4-tetrahydroisoquinoline (THIQ) pendant, behave as partial KOR agonists. As shown in Figure

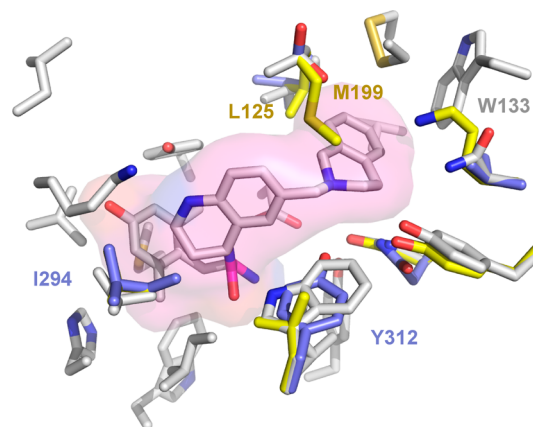


Figure 4. Overlay of **10k** in the MOR, DOR, and KOR active sites. Gray, yellow, and purple residues correspond to MOR, DOR, and KOR.

4, **10k** fits in the KOR active site but clashes slightly with I294 (and thus displays lower efficacy compared with MOR). Additionally, the THIQ nitrogen of **10k** is positioned to make a polar contact with Y312, a residue unique to the KOR binding pocket at this position, which may account for the high affinity of **10k** and **10m** for KOR. The MOR agonist/KOR agonist mixed-efficacy profile has shown promise as a treatment for drug dependence, specifically cocaine addiction,^{31–33} and an additional SAR study on MOR/KOR agonist peptides has recently been reported.³⁴ Further substitutions on the THIQ pendant will have to be explored to fully optimize this profile, particularly for the purpose of improved potency at KOR.

In Vivo Studies. On the basis of their favorable in vitro profiles, compounds **10j**, **10k**, **10m**, and **10n** were chosen for in vivo studies. The effects of **10j**, **10k**, **10m**, and **10n** were compared with those of the lead compound by two-way analysis of variance with Tukey's multiple comparisons post hoc test. A significant interaction ($F(12,76) = 8.7, p < 0.0001$) and significant main effects of dose ($F(3,76) = 82.7, p < 0.0001$) and compound ($F(4,76) = 24.6, p < 0.0001$) were found. In the mouse WWTW assay (Figure 5), our benzyl

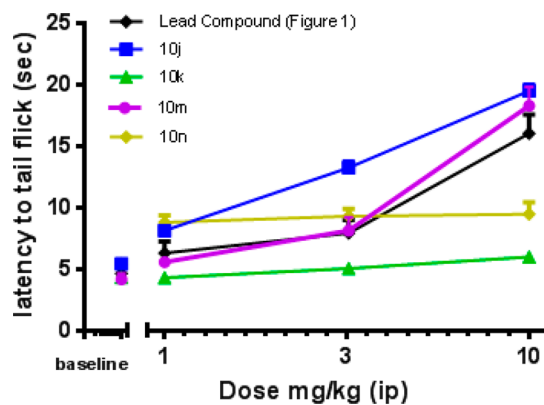


Figure 5. Cumulative antinociceptive dose–response curves for compounds **10j**, **10k**, **10m**, and **10n** in the mouse WWTW assay after intraperitoneal administration ($n = 3–6$). Data are plotted as mean \pm SEM.

pendant lead compound and compounds **10j** and **10m** were fully efficacious and produced dose-dependent increases in latency to tail flick, with 3.2 mg/kg (at least $p < 0.05$) and 10 mg/kg ($p < 0.001$) significantly increasing the latency time compared with the baseline. **10m** was not statistically different from the lead compound, but **10j** produced slightly higher tail flick latencies at 3.2 mg/kg ($p < 0.001$) and 10 mg/kg ($p < 0.05$) compared with the lead compound. It is interesting to note that **10k** (which lacks only the *N*-acetyl group of **10m**) and **10n** (which is the *N*-acetylated counterpart of **10j**) did not significantly increase the tail flick latency above baseline levels up to a dose of 10 mg/kg. To determine the duration of action of compounds **10j** and **10m**, tail withdrawal latencies were measured at intervals following the administration of the cumulative 10 mg/kg dose (Figure 6). Compounds **10j** and **10m** showed a full antinociceptive response for 200 min before returning to baseline. Compared with the lead compound (Figure 1a), these compounds both displayed a much longer duration of action after intraperitoneal injection.

In an effort to explain the unpredictable in vivo results for these structurally similar analogues, compounds **10j**, **10k**, and **10m** were screened to determine their plasma stabilities, and all

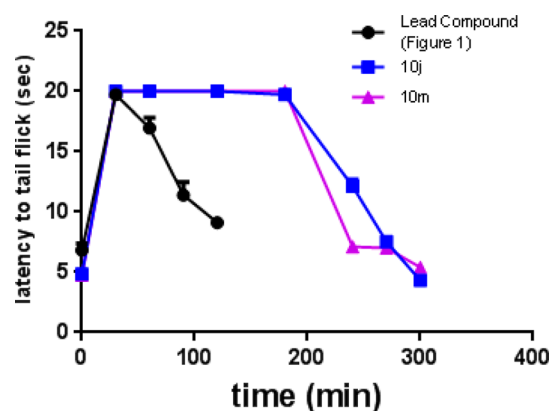


Figure 6. Time courses of antinociceptive response for compounds **10j** and **10m** in the mouse WWTW assay after intraperitoneal administration of a cumulative dose of 10 mg/kg.

were found to be completely stable after 30 min at 37 °C (99.6, 100.3, and 95.3 mean % remaining, respectively, after 30 min compared with the positive control eucatropine (43.2%)). There also appears to be no correlation between the predicted clogP values for these analogues (Table 1) and the observed in vivo data. While the origin of the disparate in vivo results is unclear, differences in first-pass metabolism after intraperitoneal administration³⁵ may be a contributing factor. To this end, additional synthetic and pharmacokinetic studies will need to be performed to shed light on how these subtle structural differences can have such a profound effect on the bioavailability of this scaffold.

CONCLUSIONS

We have described a series of opioid peptidomimetics with chemically diverse substitutions at the 6 position of the THQ scaffold and have shown that changes in both the steric and electronic characteristics of the pendant can have profound impacts on receptor selectivity for both binding and efficacy. Intermediate **3**, which is relatively simple to synthesize and can be produced on a multigram scale, represents a valuable building block for the expedient synthesis of a wide range of opioid small molecules and makes possible the incorporation of diverse and readily available side chains (through either Suzuki coupling or S_N2 substitution) that have not yet been explored in traditional opioid ligands. Compounds **10j** and **10m** also display promise in vivo, with efficacy and duration of action comparable to those of morphine, and improve upon the duration of action of our original lead.

METHODS

General Synthetic Methods. All of the reagents and solvents were obtained from commercial sources and used without additional purification. Reactions were carried out in anhydrous solvents under an inert atmosphere unless otherwise specified. Suzuki couplings were performed in a Discover S-class (CEM) microwave reactor in a closed vessel with a maximum power input of 300 W. Flash column chromatography was carried out using P60 silica gel (230–400 mesh). Purification of final compounds was performed using a Waters semipreparative HPLC instrument with a Vydac protein and peptide C18 RP column, using a linear gradient of 10% solvent B (0.1% TFA in acetonitrile) in solvent A (0.1% TFA in water) to 60% solvent B in solvent A at a rate of 1% per minute. UV absorbance was monitored at 230 nm. The purities of synthesized compounds were determined on a Waters Alliance 2690 analytical HPLC instrument with a Vydac protein and peptide C18 RP column, using a linear gradient of 0%

solvent B in solvent A to 45% solvent B in solvent A in 45 min, measuring the UV absorbance at 230 nm. The purities of the final compounds used for testing were $\geq 95\%$ as determined by HPLC. ^1H NMR, ^{13}C NMR, and ^{19}F NMR data were obtained on either a 400 or 500 MHz Varian instrument. In CDCl_3 , the chemical shifts were referenced to tetramethylsilane (TMS). If the TMS peak was not visible in the ^{13}C NMR spectrum, the chemical shifts were referenced to the solvent peak (δ 77.16). Samples in CD_3OD were unreferenced. Mass spectral analysis was performed using an Agilent 6130 LC–MS instrument in positive mode.

In Vitro Assays. Binding affinity (K_i) was measured by the competitive displacement of [^3H]diprenorphine (a nonselective opioid antagonist) in C6 cells stably expressing MOR or DOR or in Chinese hamster ovary (CHO) cells stably expressing KOR. In vitro potencies (EC_{50}) and efficacies (as maximal % stimulation) were obtained by agonist-stimulated [^{35}S]GTP γS binding in the same cell types using previously described protocols.^{21,29,36} To determine the DOR antagonist activity of **10m**, a concentration–response curve for DPDPE was obtained using the [^{35}S]GTP γS binding assay in C6 cells expressing DOR in the presence or absence of 30 nM compound **10m**, as previously described.²¹ The ratio of EC_{50} values of DPDPE in the presence and absence of **10m** was determined to provide the dose ratio. The antagonist affinity constant K_e for **10m** was calculated using the equation $K_e = [\text{10m}]/(\text{DR} - 1)$, where DR is the dose ratio of agonist in the presence and absence of **10m**. All of the concentration–response curves were analyzed using GraphPad Prism (La Jolla, CA).

Animals. Adult male C57BL/6 mice, purchased from Harlan Laboratories (Indianapolis, IN, USA) and weighing between 20 and 30 g at 8–16 weeks old, were used for the described experiments. Mice were group-housed and had free access to food and water at all times. Experiments were conducted in the housing room, which was maintained on a 12 h light/dark cycle (with lights on at 0700). Each mouse was used only once, and experiments were conducted between 9 am and 5 pm. Studies were performed in accordance with the University of Michigan Committee on the Use and Care of Animals and the Guide for the Care and Use of Laboratory Animals.³⁷

Antinociception. Each compound was dissolved in sterile saline and administered by intraperitoneal injection in a volume of 10 mL/kg of body weight. Antinociceptive effects were evaluated in the WWTW assay. Tail withdrawal latencies were determined by briefly placing a mouse into a plastic, cylindrical restrainer and putting 2–3 cm of the tail tip into a water bath maintained at 50 °C. The latency to tail withdrawal or rapidly flicking the tail back and forth was recorded with a maximum cutoff time of 20 s. If the mouse did not remove its tail by the cutoff time, the experimenter removed its tail from the water to prevent tissue damage.

Acute antinociceptive effects were determined using a cumulative dosing procedure. Each animal received an intraperitoneal injection of saline, and then 30 min later the baseline withdrawal latencies (3–6 s) were recorded. Following baseline determinations, increasing cumulative doses of the test compound were given intraperitoneally at 30 min intervals. Thirty minutes after each injection, the tail withdrawal latency was measured as described above.

Plasma Stability. Plasma stability was assessed by Quintara Discovery (San Francisco, CA). Mouse plasma (K2 EDTA) was obtained from BioreclamationIVT. The assay was carried out in 96-well microtiter plates. Compounds were diluted to 200 μM in DMSO and then spiked into the plasma. After mixing, samples were immediately aliquoted into three 96-well plates. The $t = 0$ plate was quenched immediately. The other two plates were incubated at 37 °C. Reaction mixtures (20 μL) contained a test compound final concentration of 1 μM . The extent of metabolism was calculated as the disappearance of the test compound compared with the 0 min control reaction incubations. Eucatropine was included as a positive control to verify the assay performance.

At each of the time points, 150 μL of quench solution (100% acetonitrile with 0.1% formic acid) with internal standard was transferred to each well. Plates were sealed, vortexed, and centrifuged at 4 °C for 15 min at 4000 rpm. The supernatant was transferred to fresh plates for LC–MS/MS analysis.

All of the samples were analyzed by LC–MS/MS using an AB Sciex API 4000 instrument coupled to a Shimadzu LC-20AD LC pump system. Analytical samples were separated using a Waters Atlantis T3 dC18 RP-HPLC column (10 mm \times 2.1 mm) at a flow rate of 0.5 mL/min. The mobile phase consisted of 0.1% formic acid in water (solvent A) and 0.1% formic acid in 100% acetonitrile (solvent B).

■ ASSOCIATED CONTENT

● Supporting Information

Experimental procedures, ^1H and ^{13}C NMR data, MS (EI) and HPLC data, X-ray crystallography data, and copies of NMR spectra. The Supporting Information is available free of charge on the ACS Publications website at DOI: 10.1021/acschemneuro.5b00100.

■ AUTHOR INFORMATION

Corresponding Author

*E-mail: him@med.umich.edu. Phone: (734) 764-8117.

Author Contributions

Synthesis was carried out by A.M.B. The research project was designed by A.M.B., H.I.M., and J.R.T. In vitro assays were carried out by N.W.G. In vivo studies were designed by J.P.A. and E.M.J. and carried out by J.P.A.

Funding

This study was supported by NIH Grant DA003910 (H.I.M., E.M.J., and J.R.T.). J.P.A. was supported by the Substance Abuse Interdisciplinary Training Program administered by NIDA (T32 DA007267) and N.W.G. by the Pharmacological Sciences Training Program administered by NIGMS (T32 GM007767).

Notes

The authors declare no competing financial interest.

■ ACKNOWLEDGMENTS

We are grateful to Dr. Irina Pogozheva for assistance with the ligand–receptor docking. We thank Tyler Trask, Evan Schramm, Aaron Chadderdon, and Chao Gao for additional in vitro studies, Dylan Kahl for additional synthetic contributions, and Brittany Van Koeveering for in vivo contributions.

■ REFERENCES

- (1) Benyamin, R., Trescot, A. M., Datta, S., Buenaventura, R., Adlaka, R., Sehgal, N., Glaser, S. E., and Vallejo, R. (2008) Opioid Complications and Side Effects. *Pain Physician* 11, S105–S120.
- (2) Ananthan, S. (2006) Opioid Ligands with Mixed μ/δ Opioid Receptor Interactions: An Emerging Approach to Novel Analgesics. *AAPS J.* 8, 119–125.
- (3) Schiller, P. W. (2010) Bi- or Multifunctional Opioid Peptide Drugs. *Life Sci.* 86, 598–603.
- (4) Hepburn, M. J., Little, P. J., Gingras, J., and Kuhn, C. M. (1997) Differential Effects of Naltrindole on Morphine-Induced Tolerance and Physical Dependence in Rats. *J. Pharm. Exp. Ther.* 281, 1350–1356.
- (5) Abdelhamid, E. E., Sultana, M., Portoghese, P. S., and Takemori, A. E. (1991) Selective Blockage of Delta Opioid Receptors Prevents the Development of Morphine Tolerance and Dependence in Mice. *J. Pharm. Exp. Ther.* 258, 299–303.
- (6) Kest, B., Lee, C. E., McLemore, G. L., and Inturrisi, C. E. (1996) An Antisense Oligodeoxynucleotide to the Delta Opioid Receptor (DOR-1) Inhibits Morphine Tolerance and Acute Dependence in Mice. *Brain Res. Bull.* 39, 185–188.
- (7) Zhu, Y., King, M. A., Schuller, A. G. P., Nitsche, J. F., Reidl, M., Elde, R. P., Unterwald, E., Pasternak, G. W., and Pintar, J. E. (1999)

Retention of Supraspinal Delta-like Analgesia and Loss of Morphine Tolerance in δ Opioid Receptor Knockout Mice. *Neuron* 24, 243–252.

(8) Li, T., Shiotani, K., Miyazaki, A., Tsuda, Y., Ambo, A., Sasaki, Y., Jinsmaa, Y., Marczak, E., Bryant, S. D., Lazarus, L. H., and Okada, Y. (2007) Bifunctional [2',6'-Dimethyl-L-tyrosine¹]endomorphin-2 Analogues Substituted at Position 3 with Alkylated Phenylalanine Derivatives Yield Potent Mixed μ -Agonist/ δ -Antagonist and Dual μ -Agonist/ δ -Agonist Opioid Ligands. *J. Med. Chem.* 50, 2753–2766.

(9) Schiller, P. W., Fundytus, M. E., Merovitz, L., Weltrowska, G., Nguyen, T. M. D., Lemieux, C., Chung, N. N., and Coderre, T. J. (1999) The Opioid μ Agonist/ δ Antagonist DIPP-NH₂[ψ] Produces a Potent Analgesic Effect, No Physical Dependence, and Less Tolerance than Morphine in Rats. *J. Med. Chem.* 42, 3520–3526.

(10) Balboni, G., Salvadoria, S., Trapella, C., Knapp, B. I., Bidlack, J. M., Lazarus, L. H., Peng, X., and Neumeyer, J. L. (2010) Evolution of the Bifunctional Lead μ Agonist/ δ Antagonist Containing the 2',6'-Dimethyl-L-tyrosine-1,2,3,4-Tetrahydroisoquinoline-3-carboxylic Acid (Dmt-Tic) Opioid Pharmacophore. *ACS Chem. Neurosci.* 1, 155–164.

(11) Ananthan, S., Saini, S. K., Dersch, C. M., Xu, H., McGlinchey, N., Giuvelis, D., Bilsky, E. J., and Rothman, R. B. (2012) 14-Alkoxy- and 14-Acyloxyppyridomorphinans: μ Agonist/ δ Antagonist Opioid Analgesics with Diminished Tolerance and Dependence Side Effects. *J. Med. Chem.* 55, 8350–8363.

(12) Bender, A. M., Clark, M. J., Agius, M. P., Traynor, J. R., and Mosberg, H. I. (2014) Synthesis and Evaluation of 4-Substituted Piperidines and Piperazines as Balanced Affinity μ Opioid Receptor (MOR) Agonist/ δ Opioid Receptor (DOR) Antagonist Ligands. *Bioorg. Med. Chem. Lett.* 24, 548–551.

(13) Daniels, D. J., Lenard, N. R., Etienne, C. L., Law, P., Roerig, S. C., and Portoghese, P. S. (2005) Opioid-Induced Tolerance and Dependence in Mice Is Modulated by the Distance between Pharmacophores in a Bivalent Ligand Series. *Proc. Natl. Acad. Sci. U.S.A.* 102, 19208–19213.

(14) Gomes, I., Fujita, W., Gupta, A., Saldanha, S. A., Negri, A., Pinello, C. E., Eberhart, C., Roberts, E., Filizola, M., Hodder, P., and Devi, L. A. (2013) Identification of a μ - δ Opioid Receptor Heteromer-Biased Agonist with Antinociceptive Activity. *Proc. Natl. Acad. Sci. U.S.A.* 110, 12072–12077.

(15) Breslin, H. J., Diamond, C. J., Kavash, R. W., Cai, C., Dyatkin, A. B., Miskowski, T. A., Zhang, S., Wade, P. R., Hornby, P. J., and He, W. (2012) Identification of a Dual δ OR Antagonist/ μ OR Agonist as a Potential Therapeutic for Diarrhea-Predominant Irritable Bowel Syndrome (IBS-d). *Bioorg. Med. Chem. Lett.* 22, 4869–4872.

(16) Mosberg, H. I., Yeomans, L., Anand, J. P., Porter, V., Sobczyk-Kojiro, K., Traynor, J. R., and Jutkiewicz, E. M. (2014) Development of a Bioavailable μ Opioid Receptor (MOPr) Agonist, δ Opioid Receptor (DOPr) Antagonist Peptide That Evokes Antinociception without Development of Acute Tolerance. *J. Med. Chem.* 57, 3148–3153.

(17) Mosberg, H. I., Yeomans, L., Harland, A. A., Bender, A. M., Sobczyk-Kojiro, K., Anand, J. P., Clark, M. J., Jutkiewicz, E. M., and Traynor, J. R. (2013) Opioid Peptidomimetics: Leads for the Design of Bioavailable Mixed Efficacy μ Opioid Receptor (MOR) Agonist/ δ Opioid Receptor (DOR) Antagonist Ligands. *J. Med. Chem.* 56, 2139–2149.

(18) Wang, C., McFadyen, I. J., Traynor, J. R., and Mosberg, H. I. (1998) Design of a High Affinity Peptidomimetic Opioid Agonist from Peptide Pharmacophore Models. *Bioorg. Med. Chem. Lett.* 8, 2685–2688.

(19) Healy, J. R., Bezawada, P., Shim, J., Jones, J. W., Kane, M. A., MacKerell, A. D., Jr., Coop, A., and Matsumoto, R. R. (2013) Synthesis, Modeling and Pharmacological Evaluation of UMB425, a Mixed μ Agonist/ δ Antagonist Opioid Analgesic with Reduced Tolerance Liabilities. *ACS Chem. Neurosci.* 4, 1256–1266.

(20) Anand, J. P., Purington, L. C., Pogozheva, I. D., Traynor, J. R., and Mosberg, H. I. (2012) Modulation of Opioid Receptor Ligand Affinity and Efficacy Using Active and Inactive State Receptor Models. *Chem. Biol. Drug Des.* 80, 763–770.

(21) Purington, L. C., Sobczyk-Kojiro, K., Pogozheva, I. D., Traynor, J. R., and Mosberg, H. I. (2011) Development and In Vitro Characterization of a Novel Bifunctional μ -Agonist/ δ -Antagonist Opioid Tetrapeptide. *ACS Chem. Biol.* 6, 1375–1381.

(22) Rankovic, Z. (2015) CNS Drug Design: Balancing Physicochemical Properties for Optimal Brain Exposure. *J. Med. Chem.* 58, 2584–2608.

(23) Anderson, K. W., and Tepe, J. T. (2002) Trifluoromethanesulfonic Acid Catalyzed Friedel–Crafts Acylation of Aromatics with β -Lactams. *Tetrahedron* 58, 8475–8481.

(24) Schmidt, R. G., Bayburt, E. K., Latshaw, S. P., Koenig, J. R., Daanen, J. F., McDonald, H. A., Bianchi, B. R., Zhong, C., Joshi, S., Honore, P., Marsh, K. C., Lee, C., Faltynek, C. R., and Gomtsyan, A. (2011) Chroman and Tetrahydroquinoline Ureas as Potent TRPV1 Antagonists. *Bioorg. Med. Chem. Lett.* 21, 1338–1341.

(25) Li, S. W., Nair, M. G., Edwards, D. M., Kisliuk, R. L., Gaumont, Y., Dev, I. K., Duch, D. S., Humphreys, J., Smith, G. K., and Ferone, R. (1991) Folate Analogues. 35. Synthesis and Biological Evaluation of 1-Deaza, 3-Deaza, and Bridge-Elongated Analogues of N¹⁰-Propargyl-5,8-dideazafolic Acid. *J. Med. Chem.* 34, 2746–2754.

(26) Tanuwidjaja, J., Peltier, H. M., and Ellman, J. A. (2007) One-Pot Asymmetric Synthesis of Either Diastereomer of *tert*-Butanesulfinyl-Protected Amines from Ketones. *J. Org. Chem.* 72, 626–629.

(27) Colyer, J. T., Anderson, N. G., Tedrow, J. S., Soukup, T. S., and Faul, M. M. (2006) Reversal of Diastereofacial Selectivity in Hydride Reductions of *N*-*tert*-Butanesulfinyl Imines. *J. Org. Chem.* 71, 6859–6862.

(28) Little, M. J., Aubry, N., Beaudoin, M., Goudreau, N., and LaPlante, S. R. (2007) Quantifying Trifluoroacetic Acid as a Counterion in Drug Discovery by ¹⁹F NMR and Capillary Electrophoresis. *J. Pharm. Biomed. Anal.* 43, 1324–1330.

(29) Harrison, C., and Traynor, J. R. (2003) The [³⁵S]GTP γ S Binding Assay: Approaches and Applications in Pharmacology. *Life Sci.* 74, 489–508.

(30) Dietis, N., Guerrini, R., Calo, G., Salvadori, S., Rowbotham, D. J., and Lambert, D. G. (2009) Simultaneous Targeting of Multiple Opioid Receptors: A Strategy To Improve Side-Effect Profile. *Br. J. Anaesth.* 103, 38–49.

(31) Bowen, C. A., Negus, S. S., Zong, R., Neumeyer, J. L., Bidlack, J. M., and Mello, N. K. (2003) Effects of Mixed-Action κ / μ Opioids on Cocaine Self-Administration and Cocaine Discrimination by Rhesus Monkeys. *Neuropsychopharmacology* 28, 1125–1139.

(32) Mello, N. K., and Negus, S. S. (2000) Interactions Between Kappa Opioid Agonists and Cocaine. Preclinical Studies. *Ann. N.Y. Acad. Sci.* 909, 104.

(33) Bidlack, J. M. (2014) Mixed Kappa/Mu Partial Opioid Agonists as Potential Treatments for Cocaine Dependence. *Adv. Pharmacol.* 69, 387–418.

(34) Bai, L., Li, Z., Chen, J., Chung, N. N., Wilkes, B. C., Li, T., and Schiller, P. W. (2014) [Dmt¹]DALDA Analogues with Enhanced μ Opioid Agonist Potency and with a Mixed μ / κ Opioid Activity Profile. *Bioorg. Med. Chem.* 22, 2333–2338.

(35) Lukas, G., Brindle, S. D., and Greengard, P. (1971) The Route of Absorption of Intraperitoneally Administered Compounds. *J. Pharm. Exp. Ther.* 178, 562–566.

(36) Traynor, J. R., and Nahorski, S. R. (1995) Modulation by μ -opioid agonists of guanosine-5'-O-(3-[³⁵S]thio)triphosphate binding to membranes from human neuroblastoma SH-SY5Y cells. *Mol. Pharmacol.* 47, 848–854.

(37) National Research Council (U.S.) Committee for the Update of the Guide for the Care and Use of Laboratory Animals (2011) *Guide for the Care and Use of Laboratory Animals*, 8th ed., National Academies Press, Washington, DC; available at <http://www.ncbi.nlm.nih.gov/books/NBK54050/>.